Journal of Hepatocellular Carcinoma

Dovepress
Taylor & Francis Group

Open Access Full Text Article

ORIGINAL RESEARCH

Can Intra-Operative Ablation-Specific Features Based on Ultrasound Fusion Imaging be Used to Predict Early Recurrence of Hepatocellular Carcinoma After Microwave Ablation: A Proof-of-Concept Study

Haiyu Kang[1,*], Zhong Liu[2,*], Bin Huang[2,*], Shuang Liang[1], Kai Yang[2], Huahui Liu[1], Minhua Lu[2], Ronghua Yan[3], Xin Chen[2], Erjiao Xu[1]

[1]Department of Medical Ultrasonics, The Eighth Affiliated Hospital of Sun Yat-sen University, Shenzhen, Guangdong Province, People's Republic of China; [2]National-Regional Key Technology Engineering Laboratory for Medical Ultrasound, Guangdong Key Laboratory for Biomedical Measurements and Ultrasound Imaging, School of Biomedical Engineering, Shenzhen University Medical School, Shenzhen, Guangdong Province, People's Republic of China; [3]Department of Radiology, Peking University Shenzhen Hospital, Shenzhen, Guangdong Province, People's Republic of China

*These authors contributed equally to this work

Correspondence: Erjiao Xu, Department of Medical Ultrasonics, The Eighth Affiliated Hospital of Sun Yat-sen University, No. 3025 Shennan Middle Road, Futian Street, Futian District, Shenzhen, Guangdong Province, 518033, People's Republic of China, Email xuerjiao@mail.sysu.edu.cn; Xin Chen, National-Regional Key Technology Engineering Laboratory for Medical Ultrasound, Guangdong Key Laboratory for Biomedical Measurements and Ultrasound Imaging, School of Biomedical Engineering, Shenzhen University Medical School, 1066 Xueyuan Road, Shenzhen, Guangdong Province, 518055, People's Republic of China, Email chenxin@szu.edu.cn

Purpose: Intra-operative factors are crucial to early recurrence of hepatocellular carcinoma (HCC) after microwave ablation (MWA), but few models have been developed based on intra-operative data to predict HCC recurrence after MWA. To quantify the intra-operative factors associated with MWA and establish an artificial intelligence (AI) model for predicting early recurrence of HCC after ablation based on contrast-enhanced ultrasound (CEUS) fusion imaging.

Patients and Methods: 79 hCC patients, who underwent MWA with one-year follow-up and intraoperative CEUS fusion imaging assessment were retrospectively included. Three classifiers (support vector machine (SVM), random forest (RF), and multilayer perceptron (MLP)) were developed to predict early HCC recurrence from CEUS fusion images. Thirteen ablation-specific features were defined and screened using minimum redundancy maximum relevance (mRMR), and leave-one-out cross-validation (LOOCV) was adopted for performance evaluation. Comparative analyses were conducted among classifiers and between a senior interventional doctor and the best classifier in terms of the area under the receiver operating characteristic curve (AUC).

Results: Of 79 eligible patients who were included, 22 were in the early-recurrence (age 60.18 ± 10.97; 20 males) and 57 were in the non-early recurrence (age 58.81 ± 10.89; 50 males). Six features were selected out by mRMR for early recurrence prediction and AUCs of three models were 0.84 (95% CI: 0.74, 0.94) 0.79 (95% CI: 0.69, 0.89) and 0.77 (95% CI: 0.67, 0.88) ($p = 0.20$ and 0.23 for SVM and RF, respectively), which was significantly better than that achieved by senior doctor's assessment (AUC, 0.56; 95% CI: 0.44, 0.68; $p = 0.002$ for MLP).

Conclusion: The prediction model based on ablation-specific features using intra-operative ultrasound fusion imaging data was feasible to predict early recurrence of HCC after MWA and showed great potential in guiding the real-time adjustment of the intra-operative ablation strategy so as to achieve precise ablation.

Keywords: hepatocellular carcinoma, HCC, microwave ablation, MWA, fusion imaging, artificial intelligence AI, early recurrence prediction

Introduction

Hepatocellular carcinoma (HCC) is the sixth most prevalent cancer worldwide and ranks third in terms of cancer-related mortality.[1] Resection, liver transplantation, and local thermal ablation are three optional curative methods for the treatment of

Received: 18 December 2024
Accepted: 3 May 2025
Published: 12 May 2025

HCC, among which thermal ablation is increasingly favored because of its microinvasiveness, precise therapeutic effect, and relatively low cost.[2] Numerous clinical trials and guidelines have demonstrated that there is no difference in the overall survival time between thermal ablation and surgical resection.[2–4] However, early recurrence of HCC after ablation often occurs, and it is crucial to evaluate the risk of recurrence preoperatively or immediately after ablation such that post-ablation patients can be treated separately according to the risk evaluated and eventually improve patient outcomes.[5]

The risk of early recurrence of HCC after ablation can be assessed by conducting a manual analysis on the pre-operative factors, such as serum alpha-fetoprotein (AFP) level and microvascular invasion (MVI), all of which have been found to be closely related to the early recurrence of HCC.[6–8] Because manual analysis may be subjective, some researchers have developed artificial intelligence (AI) models to mine MVI-associated features from medical images, such as B-mode ultrasound (BMUS) and contrast-enhanced ultrasound (CEUS) images, and combined the image features with clinical parameters, including AFP, for better prediction of HCC after ablation.[9–11] Although promising results have been achieved in these studies, they failed to consider intraoperative factors, such as the coverage of ablation to the target lesion and the 5-mm ablative margin (AM), which may also be associated with the recurrence of HCC after ablation.[12,13] A recent study has shown that incomplete ablation corresponds to a higher degree of tumor malignancy and a greater risk of recurrence,[14] suggesting the significance of intraoperative factors in predicting early recurrence of HCC after ablation.

Currently, few methods have been developed based on intraoperative factors to predict HCC recurrence after ablation, possibly because of the difficulties in evaluating intraoperative factors associated with ablation. With the advent of US fusion imaging and its increasing applications in real-time guidance of thermal ablation,[15–20] the evaluation of intraoperative factors associated with ablation has become possible and more convenient. Real-time BMUS images can be aligned to preoperative three-dimensional (3D) volumetric data, such as 3D US, computed tomography (CT), and magnetic resonance (MR) images, enabling simultaneous display of the ablation zone and target lesion on US images. For multiple rounds of ablation in one operation, BMUS imaging is often conducted during ablation for real-time guidance, whereas CEUS fusion imaging is often conducted after each round of ablation for quality control. With the help of CEUS fusion imaging for quality control, intraoperative factors, such as the completeness of the ablation as well as the coverage of 5-mm AM, could be manually assessed and quantified to predict the early recurrence risk of HCC after ablation. Notably, manual analysis of intraoperative factors from CEUS fusion images is subjective, and the accuracy of the analysis results is limited.

This study aimed to quantify the intraoperative factors associated with microwave ablation (MWA) using CEUS fusion imaging and to establish an artificial intelligence (AI) model for predicting the post-ablation early recurrence of HCC from CEUS fusion images.

Patients and Methods

Patients

This study adhered to the principles outlined in the Declaration of Helsinki guidelines and recommendations. Ethical approval was obtained from the committee board of the Eighth Hospital of Sun Yat-sen University (protocol number: ZB-KYIRB-2023-068-02) and the requirement for informed consent was waived because of the retrospective nature of the study. Patients with HCC who underwent MWA at the Eighth Affiliated Hospital of Sun Yat-sen University between April 2020 and December 2022 were screened to meet the requirements of our study (Figure 1). The inclusion criteria were as follows: (a) pathologically proven HCC; (b) immediate evaluation of ablation quality during MWA using US fusion imaging; and (c) no radiological evidence of major vascular invasion or extrahepatic metastasis. The exclusion criteria were (a) death during patient follow-up, (b) failure of US fusion imaging, and (c) incomplete imaging data or poor imaging quality. Patients' general information and laboratory test results were also collected.

Microwave Ablation

MWA was performed by a senior interventional radiologist (EJ.X) with > 10 years of experience in liver thermal ablation and ultrasound fusion imaging. Prior to MWA, CT/MR images of the patient's liver obtained one week or 3D US data were imported into the fusion imaging system using a GE Logiq E9 (General Electric, United States) ultrasound machine

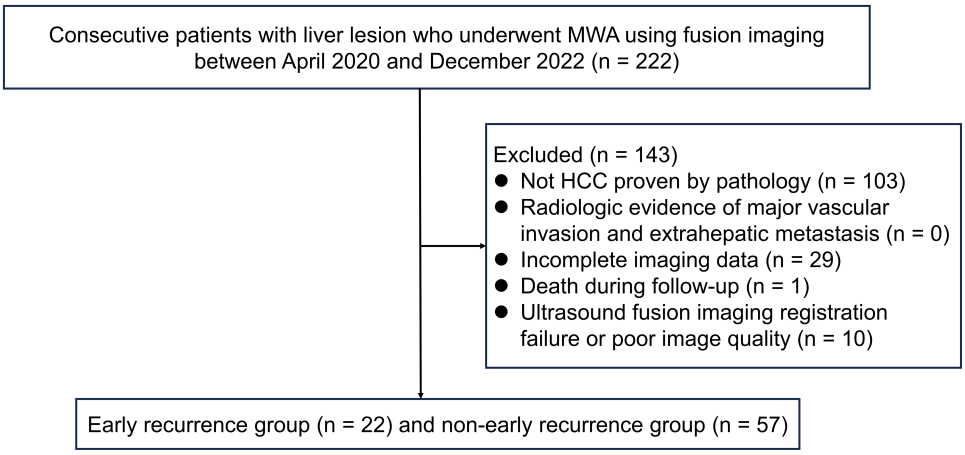

Figure 1 Flowchart of the study.
Abbreviations: HCC, hepatocellular carcinoma; MWA, microwave ablation.

equipped with a convex array probe C1-6VN (frequency 1–6MHZ), built-in volume navigation (General Electric, United States of America) ultrasound fusion imaging system, and specific ultrasound contrast imaging. The patient then underwent general anesthesia, and breathing could be suspended with the assistance of an anesthesiologist to reduce the interference of respiratory movement during registration. Subsequently, the real-time BMUS images were aligned to the preoperative 3D US/CT/MR data according to the landmarks in the liver (mainly the intrahepatic vessels) until an accurate alignment was obtained for locating the target tumor and its 5-mm AM. The MWA procedures were initiated using a 2450 MHz Great Wall microwave generator (Nanjing, China) equipped with an internal cooling microwave antenna (working power: 50 W). Fifteen minutes after completing the ablation, CEUS fusion imaging was performed to determine whether the ablation was satisfactory. Similar to BMUS fusing imaging, CEUS fusion imaging aligns CEUS frames within dynamic CEUS cine to 3D US/CT/MR data such that both the target lesion and the 5-mm AM can be outlined on each side of the CEUS-US/CT/MR fusion image. The completeness of ablation can be assessed by reviewing the CEUS-US/CT/MR fusion images. If the coverage of the ablation to the tumor and the 5-mm AM was not satisfactory, supplementary ablations were conducted, excluding cases of lesions near the liver capsule, large bile ducts, or vessels. CEUS-US/CT/MR fusion images corresponding to the last ablation time were used for the recurrence analysis.

Senior Doctor's Assessment

A senior interventional radiologist with more than 10 years of experience in thermal ablation and US fusion imaging examined the registered CEUS cine corresponding to the last time of ablation without knowing patient outcomes, and the recurrence risk was scored as follows: 0, completely; 1, mostly; 2, partially; and 3, hardly, according to a semi-quantitative visual assessment method,[21] which as defined as follows: hardly, presence of gross residual tumor; partially, ablation zone without gross residual tumor and an ablative margin < 3 mm; mostly, ablation zone without gross residual tumor and an ablative margin ≤ 3 mm to < 5 mm; and completely, ablation zone with an ablative margin ≥ 5 mm (complete ablation).

Patient Follow-Up

Each patient underwent a one-year follow-up after receiving MWA. The primary endpoint for follow-up was early recurrence of HCC, which was defined as the detection of new typical HCC lesions on contrast-enhanced CT or MR imaging.[22,23]

Model Development

A junior interventional radiologist (S. L). delineated the region of interest (ROI), which was confirmed by a senior interventional radiologist (E. J. X). Disagreements were resolved through consensus discussion. The interventional radiologists were blinded to the clinical and histopathological data. After delineating the original lesions and ablation zones, self-made ablation-specific features, including intensity- and shape-based features (Table 1), were extracted from CEUS images and binary masks. The

Table 1 Baseline Characteristics of 79 Patients Divided Into Non-Early Recurrence Group and Early Recurrence Group

Characteristics	Non-early recurrence (N=57)	Early recurrence (N=22)	p-value
Age(years)*	58.81±10.89	60.18±10.97	0.62
Gender, n(%)			>0.99
Male	50(87.72%)	20(90.91%)	
Female	7(12.28%)	2(9.09%)	
Number of nodules, n(%)			0.28
1.00	35(61.40%)	11(50%)	
2.00	15(26.32%)	6(27.27%)	
≥3	7(12.28%)	5(22.73%)	
Cirrhosis, n(%)	45(78.95%)	16(72.73%)	0.56
Hepatitis, n(%)	47(82.46%)	19(86.36%)	>0.99
Adjacent to high-risk locations, n(%)	46(80.70%)	17(77.27%)	0.76
First treatment, n(%)			0.18
Yes	22(38.60%)	5(22.73%)	
No	35(61.40%)	17(77.27%)	
Previous treatment, n	35	17	0.95
Systemic treatment	4	4	
Ablation	24	15	
Resection	13	8	
TACE	4	3	
Maximum diameter(mm)†	19.00(14.50–26.50)	21.00(16.25–30.75)	0.31
AFP(ng/mL)†	4.39(2.56–15.35)	7.54(2.46–19.85)	0.44
WBC(x10*9/L)†	5.11(4.20–6.32)	5.48(4.14–6.59)	0.92
NEU(x10*9/L)†	3.21(2.17–3.82)	2.99(2.36–3.90)	0.93
HB(g/L)†	144(129–151)	138(132–142)	0.12
PLT(x10*9/L)†	150(102–188)	140(111.5–181)	0.97
PT(s)†	13.40(13.10–14.00)	13.65(13.18–14.40)	0.40
INR †	1.04(1.01–1.11)	1.07(1.02–1.14)	0.38
TBIL(μmol/L)†	14.34(10.25–18.31)	15.75(11.69–18.79)	0.37
IBIL(μmol/L)†	11.11(7.85–15.14)	1.07(1.02–1.14)	0.49
ALB(g/L)*	38.90±4.03	39.09±4.28	0.86
γ-GT(U/L)†	48.97(28.19–73.10)	54.50(28.18–97.54)	0.35
ALT(U/L)†	26.02(19.26–33.19)	26.77(19.61–38.00)	0.80
AST(U/L)†	30.31(23.06–34.05)	29.82(22.94–41.11)	0.66

Notes: * Mean ± standard deviation; † Median (25th to 75th percentiles).
Abbreviations: TACE, transcatheter arterial chemoembolization; AFP, α-fetoprotein; WBC, white blood cell; NEU; neutrophil; HB, hemoglobin; PLT, platelet; PT, prothrombin time; INR, international normalized ratio; TBIL, total bilirubin; IBIL, indirect bilirubin; ALB, albumin; γ-GT, γ-glutamyl transpeptidase; ALT, alanine transaminase; AST, aspartate aminotransferase.

resulting features were screened using minimal-redundancy-maximal-relevance (mRMR),[24] and a machine learning algorithm, namely, a multilayer perceptron (MLP), was used to predict the probability of early recurrence of HCC. Apart from MLP, we also tested other classifiers, including random forest (RF) and support vector machine (SVM) for comparison with MLP. All models were constructed by using the scikit-learn (version 1.4.2) python package and mRMR was conducted by "pymrmr" python package (version 0.1.11). The entire pipeline is illustrated in Figure 2.

Performance Evaluation

Leave-one-out cross-validation (LOOCV) was performed to assess the performance of the prediction model. The prediction performance was measured in terms of the following: accuracy (Acc), sensitivity (Sen), specificity (Spe), positive predictive value (PPV), negative predictive value (NPV), F1 score, receiver operating characteristic (ROC) curve, and area under the ROC curve (AUC).

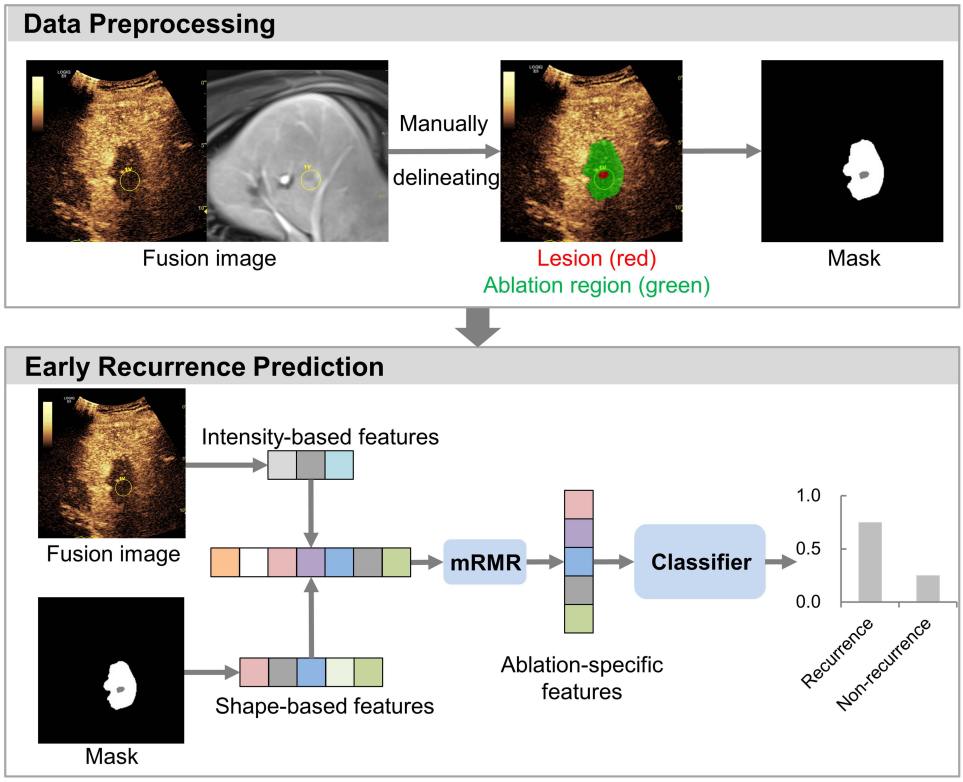

Figure 2 Pipeline of our proposed method.
Abbreviation: mRMR, minimal-redundancy-maximal-relevance.

Statistics Analysis

Continuous variables were expressed as mean ± standard deviation (SD) or median (interquartile range) and compared using Student's *t* test or Mann–Whitney *U*-test. Categorical variables pertaining to patient characteristics are expressed as numbers (n) or proportions (%) and compared using the χ^2 test or Fisher's exact test. ROC curves and corresponding AUC values were compared using the DeLong test. *P*-values were two-sided, and statistical significance was set than 0.05. All statistical analyses were performed using Statistical Package for SPSS (version 26.0).

Results

Patient Characteristics

A total of 222 patients were enrolled in our study. Of these, 143 patients, including 103 with negative pathology results, 29 with incomplete imaging data, one with death during follow-up and ten with poor image quality, were excluded. Among the included patients, 79 (mean age ± standard deviation, 59 years ± 11, 70 men) and 22 (mean age ± standard deviation, 60 years ± 11, 20 men) experienced early post-ablation recurrence with a mean follow-up time of 6.2 months, while 57 (mean age ± standard deviation, 59 years ± 11, 50 men) did not. There was no statistically significant difference in the baseline characteristics between the recurrence and non-recurrence groups (all p-values >0.05, Table 2).

Features Defined and Selected

Thirteen ablation-specific features, including six intensity- and seven shape-based features, were defined based on prior knowledge of imaging patterns regarding thermal ablation. The six intensity-based features were skewness, kurtosis, mean absolute deviation, robust mean absolute deviation, entropy, and energy, which were selected from the Radiomics feature set[25] in terms of their potential to measure the completeness, residuality, evenness of ablation, and range of the ablation zone. The seven shape-based features were as follows: maximum diameter of the original lesion, sphericity of the ablation zone, intersection over union (IoU), and dice similarity coefficient (DSC) between the lesion and ablation

Table 2 Definition and Clinical Significance of Ablation-Specific Features

Features	Definition	Clinical significance
Completeness	Completeness measures the asymmetry of the distribution of values about the mean value.	If the hyperthermia treatment is sufficient and the ablation region is not enhanced, all pixel values should be 0, the peak should be left skewed, and the completeness value should be large.
Residuality	Residuality is a measure of the "peakedness" of the distribution of values in the image ROI.	When there exists residual lesion, the enhancement of residual foci may be weak, which is easy to neglect in visual observation. The less residual foci are, the more pixels are clustered around 0, showing a peak distribution with a large residuality value.
Ablation evenness	Ablation evenness is the mean distance of all intensity values from the mean value of the image array.	Ablation evenness reflects the entire distribution of the ablation region. The image of the incomplete ablation has more non-zero pixel values, and the distribution of zero values is uneven, so the feature values should be large.
Robust ablation evenness	Robust ablation evenness is the mean distance of all intensity values from the mean value calculated on the subset of image array with gray levels in between, or equal to the 10th and 90th percentile.	Robust ablation evenness reflects the robust distribution of the ablation region. The image of the incomplete ablation has more non-zero pixel values, and the distribution of zero values is uneven, so the feature values should be large.
Entropy	Entropy specifies the uncertainty/randomness in the image values. It measures the average amount of information required to encode the image values.	It is related to the range of pixel value distribution. The more non-perfused areas there are, the more concentrated the pixel values are around zero, resulting in lower entropy, which indicates complete ablation.
Energy	Energy is a measure of the magnitude of pixel values in an image. A larger value implies a greater sum of the squares of these values.	It is also related to the range of the ablation area and pixel values. A larger energy indicates a larger ablation range and more perfused areas.
Maximum diameter(lesion)	Maximum diameter is defined as the largest diameter of original lesion.	Maximum diameter reflects the volume of tumor to some extent which is related to the recurrence.
Sphericity	Sphericity is the ratio of the perimeter of the tumor region to the perimeter of a circle with the same surface area as the tumor region.	The higher the sphericity is, the more regular the tumor shape is, and the easier to achieve complete ablation.
Ablation extendedness-1	Equal to the intersection over union between original lesion area and ablation area	The ablation extendedness should be less than 1, and the smaller it is, the larger the ablation boundary expansion is.
Ablation extendedness-2	Equal to the Dice similarity coefficient between original lesion area and ablation area	Similar to ablation extendedness-1.
Minimum ablation margin	Minimum distance of ablation margin and original lesion margin	Minimum ablation margin reflects the distance between ablation and lesion margins, which is related to the recurrence.
Mean ablation margin	Mean distance of ablation margin and original lesion margin	Mean ablation margin reflects the entire distance between ablation and lesion margins, which is related to the recurrence.
Ablation margin standard deviance	Standard deviance of distance of ablation margin and original lesion margin	Mean ablation margin reflects the distances' variations between ablation and lesion margins, which is related to the degree of curvature of the ablation margin.

zone; minimum/mean/SD for the distance between the margins of the lesion and ablation zones, which has the capacity to measure the shape and size of the ablation zone, as well as the relationship between the location of the lesion and ablation. Among the 13 features, five, including two intensity-based features (residuality and entropy) and three shape-based features (minimum ablation margin, ablation margin standard deviance, and ablation extendedness-1), were screened out by mRMR for recurrence prediction.

Table 3 Prediction Performance of Different Models and Doctor

Model	Sen	Spe	Acc	PPV	NPV	F1 score	Threshold	AUC(95% CI)	p-value	
MLP	0.73	0.89	0.85	0.73	0.89	0.73	0.46	0.84(0.74, 0.94)		
SVM	0.82	0.68	0.72	0.50	0.91	0.62	0.21	0.79(0.69, 0.89)	0.20	
RF	0.82	0.65	0.70	0.47	0.90	0.60	0.29	0.77(0.67, 0.88)	0.23	0.64
Doctor	0.45	0.67	0.61	0.34	0.76	0.39	–	0.56(0.44, 0.68)	**<0.001**	–

Notes: The values were shown in bold since their differences are statistically significant.
Abbreviations: Sen, sensitivity; Spe, specificity; Acc, accuracy; PPV, positive predictive value; NPV, negative predictive value; AUC, area under curve; MLP, multilayer perceptron; SVM, support vector machine; RF, random forest.

Prediction Performance

Among the three classifiers, MLP provided the best performance (AUC, 0.84; 95% CI 0.74–0.94 vs AUCs: 0.79; 95% CI, 0.69–0.89; and 0.77, 95% CI 0.67–0.88, for SVM and RF, respectively), but there was no statistically significant difference between the AUC values of MLP and those of the other classifiers (all p-values > 0.05). Moreover, the MLP prediction model significantly outperformed the senior interventional radiologist's assessment (AUCs: 0.84, 95% CI 0.74–0.94 vs 0.56, 95% CI 0.44–0.68. for the former and latter groups, respectively; $p = 0.002$). The quantitative results of different classifiers, together with those obtained by the interventional radiologist's assessment, are summarized in Table 3, and the corresponding ROC curves are presented in Figure 3. To further demonstrate the superiority of the model over interventional radiologists' assessments, Figure 4 shows a non-recurrence case misdiagnosed by the interventional radiologist but

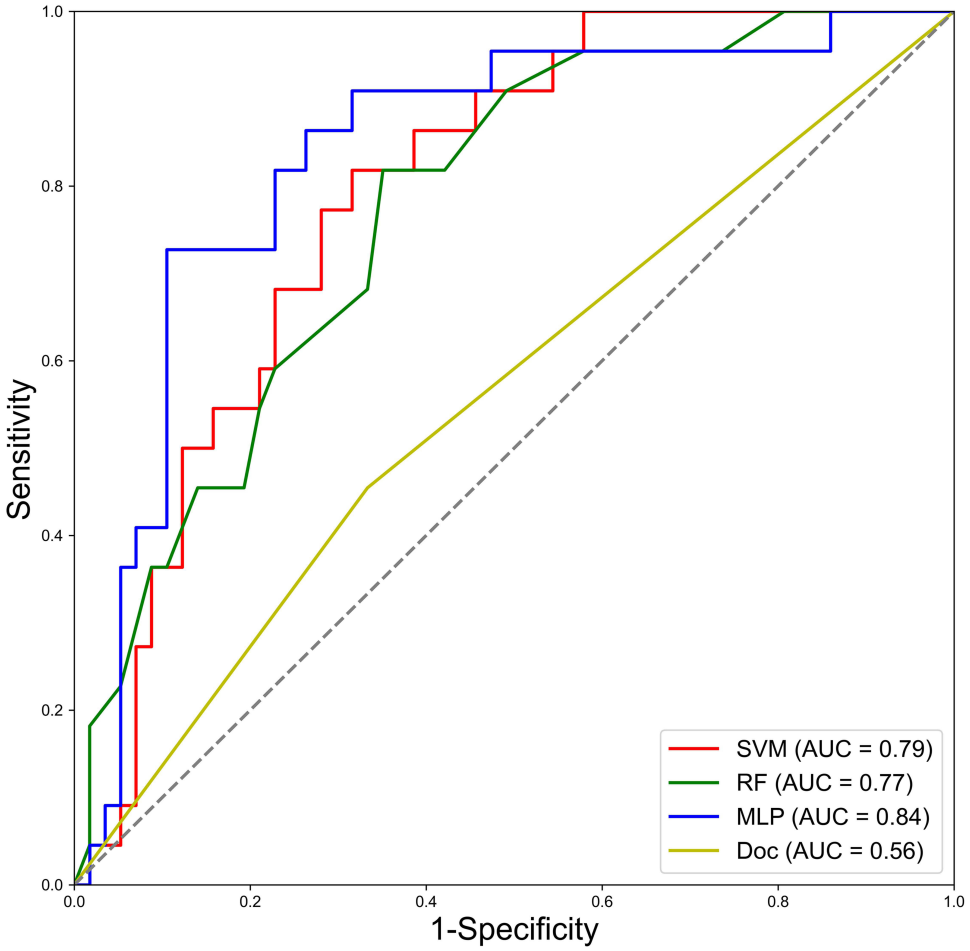

Figure 3 ROC curves of three machine learning models and doctor to predict early recurrence of hepatocellular carcinoma.
Abbreviation: ROC, receiver-operating-characteristic.

https://doi.org/10.2147/JHC.S512926

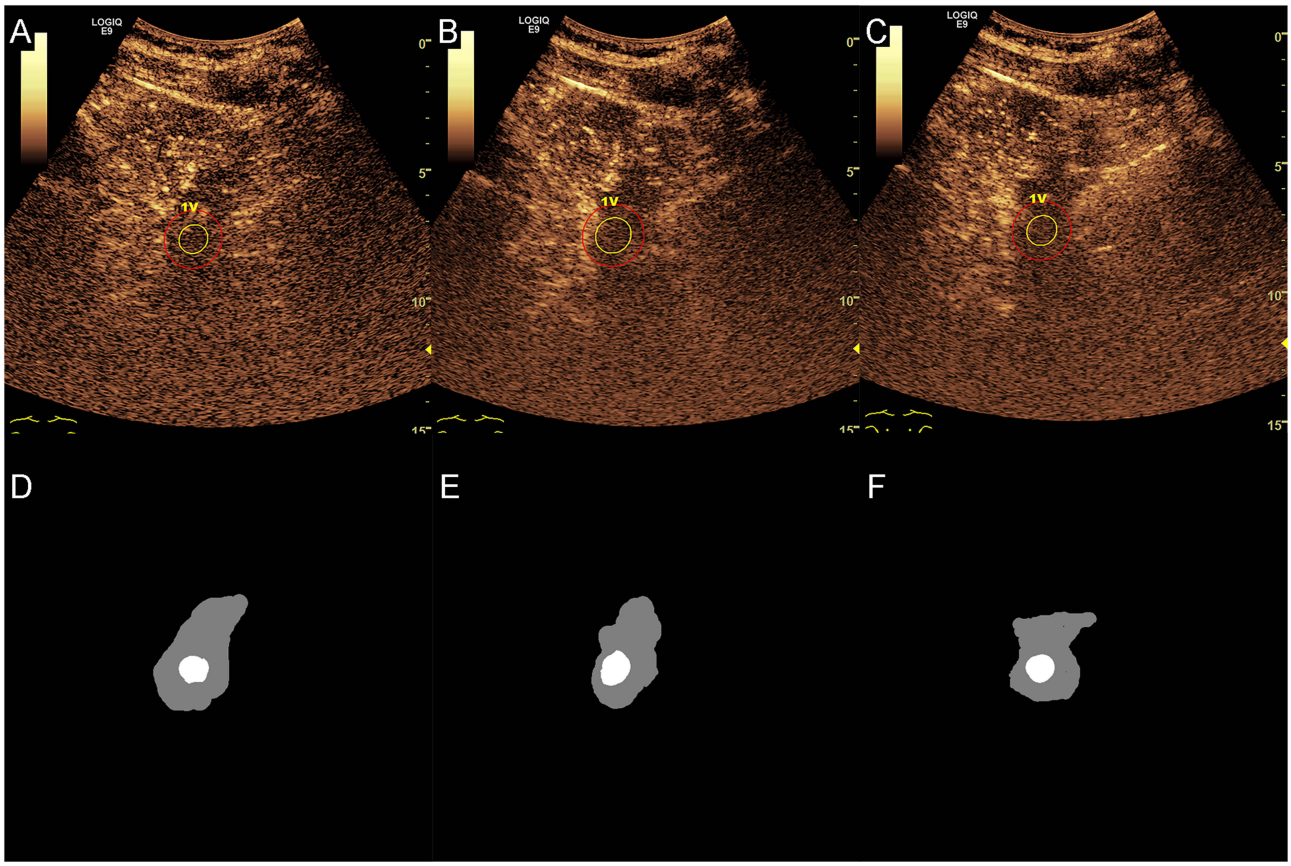

Figure 4 A non-recurrence case (42, man) was assessed as low risk of early recurrence by model but high risk by doctor. Complete ablation achieved basically in two sections but partial coverage of the ablation to the 5-mm ablation margin of the target lesion was found in (**B**). (**A**) upper pole section; (**B**) maximum diameter section; (**C**) lower pole section; (**D–F**) masks of the ablation zone and original tumor zone.

correctly diagnosed by the model. In this case, a high recurrence risk score of 2 was given by the senior interventional radiologist because of the partial coverage of the ablation to the 5-mm AM of the target lesion reflected by the fusion images, whereas the model predicted non-recurrence by processing the quantitative ablation-specific features in the fusion images. Figure 5 shows a recurrence case that was misdiagnosed by the interventional radiologist but correctly diagnosed by the model. According to the complete coverage of the ablation to the 5-mm AM of the target lesion, a low recurrence risk score of 0 was given by the doctor; however, the model predicted recurrence based on ablation-specific features. The five selected ablation-specific features for the two cases are listed in Table 4.

Discussion

This proof-of-concept study proposed an AI model for predicting the early recurrence of HCC after ablation using intraoperative CEUS fusion images. In a cohort of 79 patients who underwent MWA and one-year follow-up, the best classifier achieved an AUC value of 0.84, 95% CI 0.74–0.94, which was significantly higher than that of the senior interventional radiologist's assessment (AUC: 0.56, 95% CI 0.44–0.68; $p = 0.002$).

Few studies have used intraoperative data to predict the recurrence of HCC after ablation. Benefiting from the US fusion imaging, an AI model driven by intraoperative imaging data for early recurrence prediction was successfully constructed in this study. To the best of our knowledge, this study is the first attempt to use intraoperative CEUS fusion images to develop AI models to predict the early recurrence of HCC after MWA. In addition to preoperative data, several studies have used postoperative data for recurrence analysis.[26,27] From the viewpoint of clinical significance, the preoperative information did not represent the operation itself, and the post-ablation data provided minimal value for early management. It should be always remembered that the most critical factor affecting the recurrence rate is the

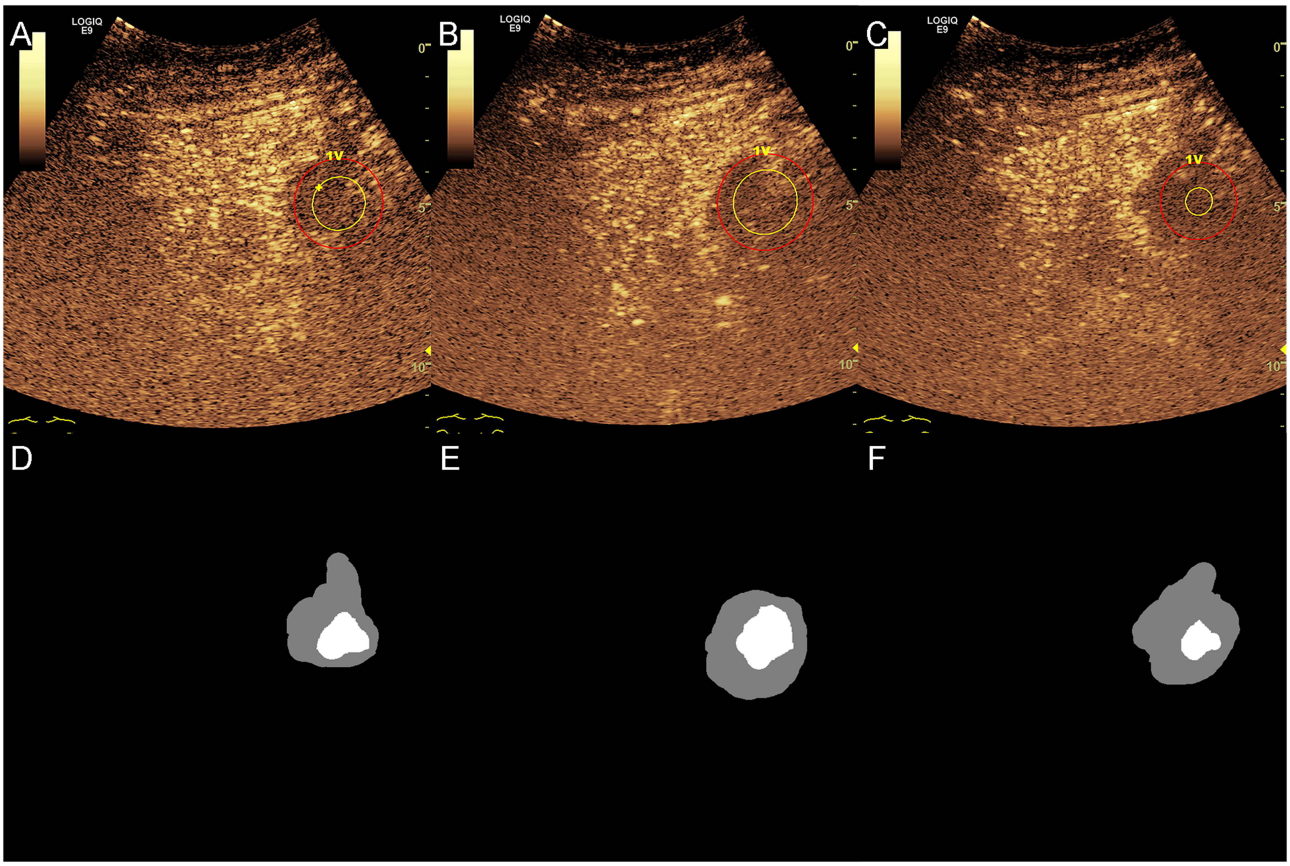

Figure 5 A recurrence case (63, man) was assessed as high risk of early recurrence by model but low risk by doctor. Complete ablation achieved basically in three sections. (**A**) upper pole section; (**B**) maximum diameter section; (**C**) lower pole section; (**D**–**F**) masks of the ablation zone and original tumor zone.

thermal ablation itself. However, the aim of model development was not to replace the models developed based on preoperative data. Rather, the proposed model may be jointly used with those developed based on preoperative data for a more accurate prediction of early recurrence of HCC after MWA.

The prediction pipeline comprises feature extraction, selection, and classification components. Regarding feature extraction, instead of the aimless use of imaging features, ablation-specific features were defined or carefully chosen from the existing feature set according to our prior knowledge of the imaging patterns of ablation. The benefits are twofold. First, defining or selecting features according to prior knowledge may prevent the influence of irrelevant features on prediction, particularly for predictions on small-scale datasets. Second, the features defined or selected were linked well to clinical significance, making the AI model interpretable In this study, five features, including two intensity-based features (residuality and entropy) and three shape-based features (minimum ablation margin, ablation margin standard deviance, and ablation extendedness-1), were screened using mRMR for recurrence prediction. All features

Table 4 Five Selected Features of the Two Cases from Three Different Sections

Features	Case1			Case2		
	Section1	Section2	Section3	Section1	Section2	Section3
Residuality	6.48	11.27	12.31	5.91	7.42	9.16
Minimum ablation margin	30.00	3.00	21.93	11.00	24.00	34.00
Entropy	0.99	1.00	0.99	0.78	0.46	0.62
Ablation margin standard deviance	5.26	13.08	5.61	14.31	12.51	13.26
Ablation extendedness-1	0.10	0.17	0.11	0.22	0.25	0.06

https://doi.org/10.2147/JHC.S512926

were well-linked to their clinical significance. This may provide several hints to senior or less experienced clinicians to improve their diagnosis. For instance, although the minimum AM of 5-mm has gradually been accepted,[12,13] this may not be the only factor to be considered by clinicians for evaluating the early recurrence of HCC, which indicates that using a single indicator is not an optimal method, so we should take multiple features into account rather than focusing on one feature.

In clinical practice, the proposed model can be used to customize strategies for patient follow-up. For patients with early recurrence gauged by the model, a more aggressive follow-up schedule could be used, such as by conducting examinations using CT/MRI or other highly sensitive imaging techniques more frequently. Moreover, the proposed model can be used as an auxiliary tool for determining the ablation endpoint for each operation. After performing CEUS fusion imaging for each round of ablation during the operation, the CEUS data could be first handled by the model to predict recurrence, and the results could be referenced by clinicians during the review of the CEUS data. By doing so, the quality of the ablation operation can be enhanced, eventually improving the patient outcomes. According to the results, the MLP model performed the best in AUC, but there was no statistically significant difference between it and the other two classifiers. Early recurrence of HCC requires early detection and timely treatment to improve the prognosis of patients. Therefore, in addition to paying attention to the AUC, we should attach importance to the sensitivity of the early recurrence prediction model. The sensitivities of the MLP, SVM, and RF models are 0.73, 0.82, and 0.82 respectively. Therefore, from this perspective, the SVM and RF models may be more suitable for future clinical applications.

As for the reasons for the doctor's misjudgment in Figures 4 and 5, interventional radiologists mainly judge the prognosis by evaluating the coverage of the tumor and the safety margin by the non-enhanced ablation zone. However, there is a certain degree of subjectivity in their evaluation of images. For example, interventional radiologists may misjudge some hyperechoic areas caused by gas and ablated tissue after ablation as enhanced regions and wrongly consider the ablation as insufficient. Or during the ablation of lesions in risk locations, the operator may believe that complete ablation has been achieved based on CEUS evaluation, but early recurrence occurs as predicted by the model. Therefore, it is not sufficient to merely visually observe whether the 5 mm safety margin has been reached by ablation. Our study utilized the intra-operative fusion imaging data to extract quantitative ablation-specific features for a comprehensive evaluation of the ablation zone, which can reduce such misjudgments.

Our study had several limitations. First, owing to its retrospective nature and single-center/small-sized dataset, study bias is inevitable As for the nature of this proof-of-concept study, the feasibility of a new concept of ablation-specific features was proven using this small-sized dataset. In addition, the value of ablation-specific features in clinical practice has been validated using machine learning. Second, the proposed model could only be used for predicting early recurrence of HCC within one-year rather than long-term prognosis prediction. We will conduct long-term follow-up of the patients included in this study. Finally, the robustness of ablation-specific features needs to be further verified using an external validation dataset. However, fusion imaging techniques are performed less frequently in other institutions; therefore, it is difficult to obtain an ideal external validation set. In addition, the predictive effects of different combinations of ablation-specific features and multimodal data from other periods need to be explored.

Conclusion

In conclusion, the prediction model built on ablation-specific features proved the feasibility of the new concept of ablation-specific features in predicting the early recurrence of HCC after MWA. Explainable ablation-specific features may break the AI "black box" to some extent. In clinical practice, the evaluation of the ablation margin based on ablation-specific features may reduce the operator's experience dependence, guide junior doctors to achieve the same sufficient ablation effect during the operation, and at the same time overcome the subjectivity of visual evaluation, supplementing the traditional 5mm safety margin method. In the future, it is highly necessary to attempt to validate the scientific nature of the ablation-specific features on a larger dataset. Additionally, with the development of deep learning, more discriminative feature combinations can be explored, and a comparative study between the models based on deep learning features and those based on ablation-specific features will be our next research plan.

Patient Data Confidentiality Statement

The Eighth Hospital of Sun Yat-sen University respects and safeguards the privacy and confidentiality of patient information. Although patient consent for the review of their medical records was not required, we are committed to maintaining the highest standards of data protection.

This research conducted at the Eighth Hospital of Sun Yat-sen University is a retrospective study, not an interventional one. Our research approach was designed to minimize any potential risks to patient privacy from the outset.

In the process of data collection, all patient - related data were anonymized. Specifically, patient identifiers such as names, medical record numbers, dates of birth, and addresses were systematically removed or encrypted. This ensures that individual patients cannot be identified through the data used in our study.

When dealing with medical images, we employed strict procedures to guarantee that no personal information was involved. Our image processing techniques were focused solely on extracting relevant medical features for research purposes. For example, any text or markings on the images that could potentially identify the patient were carefully erased or masked.

Moreover, access to the patient data was restricted. Only authorized researchers directly involved in this study had access to the data, and they were all bound by strict confidentiality agreements. These agreements explicitly state that they are not allowed to disclose any patient - related information under any circumstances.

The data storage system was also designed with security in mind. It is a password - protected and encrypted system, which further safeguards the confidentiality of patient data. Regular backups are made to prevent data loss, and the backup storage also adheres to the same high - level security standards.

We are committed to upholding the highest standards of patient data confidentiality throughout the entire research process. By implementing these comprehensive measures, we ensure that the rights and privacy of our patients are fully protected while still enabling valuable medical research to be conducted.

Funding

This study has received funding by the National Natural Science Foundation of China (82272011, 82272014, 82327804 and 61901282), the Natural Science Foundation of Guangdong Province, China (2022A1515012155, 2024A1515010513), the Shenzhen Technology Program Science and Project (JCYJ20220530160208018, JCYJ20230807095102005), Shenzhen Basic Science Research (Key Program) (JCYJ20220818095612027), Shenzhen Basic Science Research (JCYJ20210324093006017).

Disclosure

Haiyu Kang, Zhong Liu and Bin Huang are co-first authors for this study. Xin Chen and Erjiao Xu are co-senior authors for this study. The author(s) report no conflicts of interest in this work.

References

1. Chen R, Hou B, Zhou Y, et al. Recurrence after percutaneous radiofrequency ablation of hepatocellular carcinoma: analysis of the pattern and risk factors. *Front Oncol*. 2023;13:1018715. doi:10.3389/fonc.2023.1018715
2. Reig M, Forner A, Rimola J, et al. BCLC strategy for prognosis prediction and treatment recommendation: the 2022 update. *J Hepatol*. 2022;76 (3):681–693. doi:10.1016/j.jhep.2021.11.018
3. Jiang L, Yan L, Wen T, et al. Comparison of outcomes of hepatic resection and radiofrequency ablation for hepatocellular carcinoma patients with multifocal tumors meeting the Barcelona-Clinic Liver Cancer stage A classification. *J Am Coll Surg*. 2015;221(5):951–961. doi:10.1016/j.jamcollsurg.2015.08.009
4. Doyle A, Gorgen A, Muaddi H, et al. Outcomes of radiofrequency ablation as first-line therapy for hepatocellular carcinoma less than 3 cm in potentially transplantable patients. *J Hepatol*. 2019;70(5):866–873. doi:10.1016/j.jhep.2018.12.027
5. Liu W, Zou R, Wang C, et al. Microwave ablation versus resection for hepatocellular carcinoma within the Milan criteria: a propensity-score analysis. *Ther Adv Med Oncol*. 2019;11:1758835919874652. doi:10.1177/1758835919874652
6. Lee S, Kang TW, Song KD, et al. Effect of microvascular invasion risk on early recurrence of hepatocellular carcinoma after surgery and radiofrequency ablation. *Ann Surg*. 2021;273(3):564–571. doi:10.1097/SLA.0000000000003268
7. Mazzaferro V, Llovet JM, Miceli R, et al. Predicting survival after liver transplantation in patients with hepatocellular carcinoma beyond the Milan criteria: a retrospective, exploratory analysis. *Lancet Oncol*. 2009;10(1):35–43. doi:10.1016/S1470-2045(08)70284-5
8. Luo B, Liu L, Bi J, Bao S, Zhang Y. Role of the pre- to postoperative alpha-fetoprotein ratio in the prognostic evaluation of liver cancer after radiofrequency ablation. *Int J Biol Markers*. 2022;37(3):306–313. doi:10.1177/03936155221101075

9. Wu JP, Ding WZ, Wang YL, et al. Radiomics analysis of ultrasound to predict recurrence of hepatocellular carcinoma after microwave ablation. *Int J Hyperthermia*. 2022;39(1):595–604. doi:10.1080/02656736.2022.2062463
10. Ni Z, Wu B, Li M, et al. Prediction model and nomogram of early recurrence of hepatocellular carcinoma after radiofrequency ablation based on logistic regression analysis. *Ultrasound Med Biol*. 2022;48(9):1733–1744. doi:10.1016/j.ultrasmedbio.2022.04.217
11. Zhong X, Peng J, Xie Y, et al. A nomogram based on multi-modal ultrasound for prediction of microvascular invasion and recurrence of hepatocellular carcinoma. *Eur J Radiol*. 2022:151.
12. Laimer G, Schullian P, Jaschke N, et al. Minimal ablative margin (MAM) assessment with image fusion: an independent predictor for local tumor progression in hepatocellular carcinoma after stereotactic radiofrequency ablation. *Eur Radiol*. 2020;30(5):2463–2472. doi:10.1007/s00330-019-06609-7
13. Li FY, Li JG, Wu SS, et al. An optimal ablative margin of small single hepatocellular carcinoma treated with image-guided percutaneous thermal ablation and local recurrence prediction base on the ablative margin: a multicenter study. *J Hepatocell Carcinoma*. 2021;8:1375–1388. doi:10.2147/JHC.S330746
14. Su T, Huang M, Liao J, et al. Insufficient radiofrequency ablation promotes hepatocellular carcinoma metastasis through N6-methyladenosine mRNA methylation-dependent mechanism. *Hepatology*. 2021;74(3):1339–1356. doi:10.1002/hep.31766
15. Minami Y, Minami T, Hagiwara S, et al. Ultrasound-ultrasound image overlay fusion improves real-time control of radiofrequency ablation margin in the treatment of hepatocellular carcinoma. *Eur Radiol*. 2018;28(5):1986–1993. doi:10.1007/s00330-017-5162-8
16. Li K, Su ZZ, Xu EJ, Ju JX, Meng XC, Zheng RQ. Improvement of ablative margins by the intraoperative use of CEUS-CT/MR image fusion in hepatocellular carcinoma. *BMC Cancer*. 2016;16:277. doi:10.1186/s12885-016-2306-1
17. Ahn SJ, Lee JM, Lee DH, et al. Real-time US-CT/MR fusion imaging for percutaneous radiofrequency ablation of hepatocellular carcinoma. *J Hepatol*. 2016:S0168827816305049.
18. Ma QP, Xu EJ, Zeng QJ, et al. Intraprocedural computed tomography/magnetic resonance-contrast-enhanced ultrasound fusion imaging improved thermal ablation effect of hepatocellular carcinoma: comparison with conventional ultrasound. *Hepatol Res*. 2019;49(7):799–809. doi:10.1111/hepr.13336
19. Zhang T, Liang W, Song Y, Wang Z, Zhang D. Microwave ablation of colorectal liver metastases guided by US-PET/CT fusion imaging: a case report. *Adv Ultrasound Diagnosis Ther*. 2021;5(1):58–62. doi:10.37015/AUDT.2021.200002
20. Takeyama N, Mizobuchi N, Sakaki M, et al. Evaluation of hepatocellular carcinoma ablative margins using fused pre- and post-ablation hepatobiliary phase images. *Abdom Radiol*. 2019;44(3):923–935. doi:10.1007/s00261-018-1800-0
21. Yoon JH, Lee JM, Klotz E, et al. Prediction of local tumor progression after Radiofrequency Ablation (RFA) of hepatocellular carcinoma by assessment of ablative margin using pre-RFA MRI and post-RFA CT registration. *Korean J Radiol*. 2018;19(6):1053–1065. doi:10.3348/kjr.2018.19.6.1053
22. Poon RT, Fan ST, Ng IO, Lo CM, Liu CL, Wong J. Different risk factors and prognosis for early and late intrahepatic recurrence after resection of hepatocellular carcinoma. *Cancer*. 2000;89(3):500–507. doi:10.1002/1097-0142(20000801)89:3<500::AID-CNCR4>3.0.CO;2-O
23. Jung SM, Kim JM, Choi GS, et al. Characteristics of early recurrence after curative liver resection for solitary hepatocellular carcinoma. *J Gastrointest Surg*. 2019;23(2):304–311. doi:10.1007/s11605-018-3927-2
24. Hanchuan P, Fuhui L, Ding C. Feature selection based on mutual information criteria of max-dependency, max-relevance, and min-redundancy. *IEEE Trans Pattern Analysis Machine Intell*. 2005;27(8):1226–1238. doi:10.1109/TPAMI.2005.159
25. Zwanenburg A, Vallières M, Abdalah MA, et al. The image biomarker standardization initiative: standardized quantitative radiomics for high-throughput image-based phenotyping. *Radiology*. 2020;295(2):328–338. doi:10.1148/radiol.2020191145
26. Kobe A, Kindler Y, Klotz E, et al. Fusion of preinterventional MR imaging with liver perfusion CT after RFA of hepatocellular carcinoma: early quantitative prediction of local recurrence. *Invest Radiol*. 2021;56(3):188–196. doi:10.1097/RLI.0000000000000726
27. Yu SJ, Kwon JH, Kim W, et al. Initial alpha-fetoprotein response predicts prognosis in Hepatitis B-related solitary HCC patients after radiofrequency ablation. *J Clin Gastroenterol*. 2018;52(3):e18–e26. doi:10.1097/MCG.0000000000000841